Conceptual Improvement in Seismic Design of Slender Reinforced Concrete Structural Walls on Isolated Footings – A Summary

Kaustubh Dasgupta[1] and C. V. R. Murty[2]

[1] *PhD Candidate, Dept. of Civil Engineering , Indian Institute of Technology Kanpur, Kanpur, India*
[2] *Professor, Dept. of Civil Engineering , Indian Institute of Technology Kanpur, Kanpur, India*
Email: kaustubh.dasgupta@gmail.com, cvrm@iitk.ac.in

ABSTRACT :

In the current seismic design practice, capacity design of slender RC structural wall without enlarged boundary elements and on shallow footing considers plastic hinge to occur at the base of wall along with prevention of other modes of failure during strong earthquake shaking. However, the re-entrant corner of wall-footing junction is observed to incur significant damage during past earthquakes and experiments. This leads to costly seismic retrofitting of footing after earthquakes. The present study investigates a new geometric configuration at wall-footing junction concerned with smooth flow of forces from wall to footing. A structural wall from a six-storeyed RC wall-frame building with symmetric plan configuration is provided with linear and curvilinear tapered configurations at the bottom of wall. Linear elastic finite element analysis is carried out in SAP2000 program using 8-noded solid elements for modeling wall and footing, and smeared spring elements for soil flexibility. The proposed wall-footing system exhibits rigid block-type behaviour irrespective of soil flexibility. Combination of linear and curvilinear tapers ensures most favourable stress distribution and prevents damage in footing below ground level. The region of damage is located above the tapered region and this can be located above normal ground level. Strategies are presented to suitably proportion the tapered wall-footing monolith.

KEYWORDS: Seismic design, RC slender wall, wall configuration, wall footing, seismic damage

1. INTRODUCTION

RC slender structural wall is an important component of lateral force resisting system of multistoreyed RC frame-wall building. During strong earthquake shaking, formation of plastic hinge at the bottom of wall is associated with irregular stress distribution and force flow in that region. Geometry of wall-footing junction significantly influences the flow of forces from wall to footing. In wall-footings, either without any taper from edge of footing to edge of wall or with marginal taper, reentrant corner of wall-footing junction causes severe stress concentration. This is likely to cause local failures of wall-footing junction region and footing, e.g., compression failure of concrete and buckling of reinforcement in past earthquake [EERI, 1987] and laboratory tests [Kotronis et. al., 2005]. Although rocking behavior of shallow footings have been investigated [Gajan and Kutter, 2008; Allotey and El Naggar, 2008], local failure at wall-footing junction has not been studied.

In this study, a new geometric configuration is proposed, in walls without enlarged boundary elements, to ensure smooth flow of forces at the bottom region and minimise seismic damage in footing. A detailed parametric study is carried out and possible strategies of proportioning discussed.

2. BUILDING DETAILS

A six-storeyed RC wall-frame building is considered in the present study with aspect ratio of

structural walls A_r (= H_w/L_w) as 4.33, where H_w and L_w are height and length of wall (Figure 1). Thickness of RC wall is taken as 0.2 m uniformly throughout its height. Design lateral forces on the wall for seismic load case are obtained as per the relevant Indian Code of Practice [IS:1893 (Part 1), 2002]. Grades of concrete and steel are taken as M25 and Fe415, respectively. Along each of the two directions X and Y, design lateral force is assumed to be shared equally by the two walls.

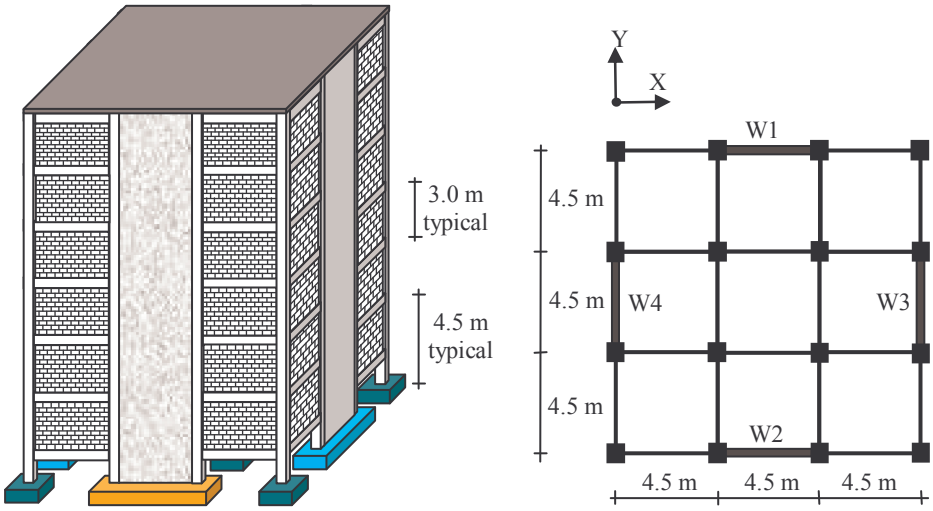

Figure 1 Six-storeyed RC frame-wall building, and typical floor plan.

3. METHODOLOGY

Isolated wall-footings are modeled using 8-noded solid elements in computer program SAP2000 [CSI, 2006] with incompatible bending modes option. Characteristic mesh size of 0.1 m was determined from mesh convergence studies [Dasgupta, 2008]. Linear elastic analysis of wall-footing system is carried out under combined vertical and lateral loads expected during actual earthquake shaking. Nodal shear and principal compressive stress demands, τ and $\sigma_{com,p}$ respectively, are monitored in the bottom D-region. These are normalised with respect to average shear stress τ_{av} in wall, and bending compressive stress σ_{bot} at bottom of footing respectively. Compression strut angles θ are normalised with respect to 90°.

Behaviour of isolated wall-footing is investigated under concentrated vertical and lateral forces. Translational degrees of freedom (DOF) are restrained at the bottom face of footing. Reentrant corner at wall-footing junction tends to draw maximum force under applied loads, and this leads to severe shear stress concentration (Figure 2a). In footing, peak τ is observed at the bottom vertically below wall-footing junction (Figure 2b). Variations of longitudinal stress in footing and principal compressive stress at wall-footing junction show possibility of flexural-shear cracking and compression failure of concrete respectively [Dasgupta, 2008]. Thus, footing requires inspection and possible strengthening after every earthquake; these may be costly and inconvenient.

4. PARAMETRIC STUDY

Based on results of preliminary study mentioned above, two different tapered configurations are investigated, namely (a) curvilinear profile with degree of curve $n_d \geq 1.0$ (Figure 3a), and (b) combined taper consisting of linear and curvilinear profiles (Figure 3b). In case (a), geometry is defined by a single curve over height of taper H_t and in case (b), by the ratio r_t (=H_{tl}/H_{tc}), where H_{tl} and H_{tc} are the heights of linear and curvilinear profiles.

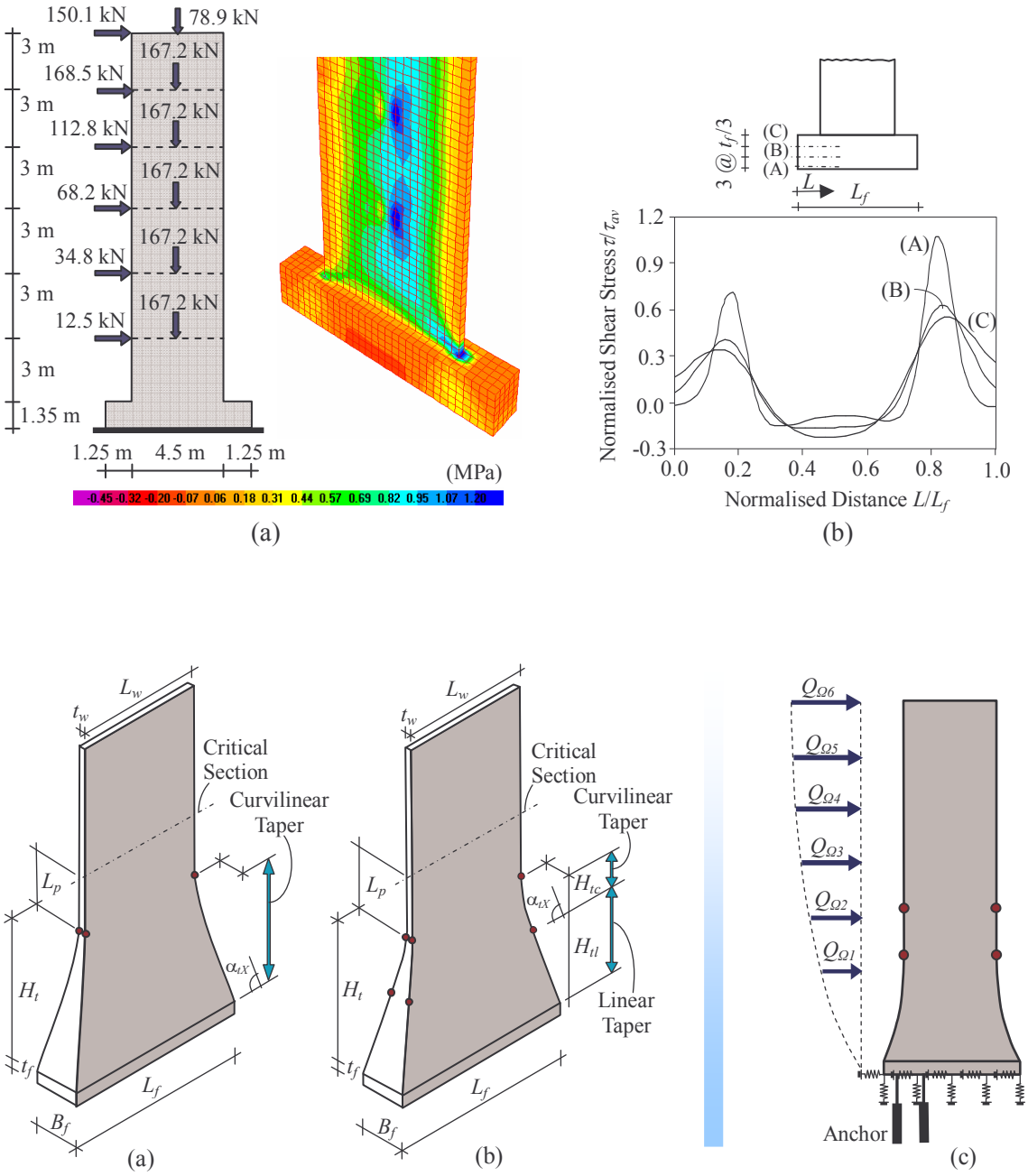

Figure 3 RC walls with (a) curvilinear and (b) combined tapered configurations; (c) applied forces during overstrength.

Critical section of design in tapered wall is taken at a distance of idealised plastic hinge length L_p above the top of taper (Figures 3a and 3b); L_p is taken as $0.5L_w$ [Paulay and Priestley, 1992]. Design and detailing are carried out against forces and moments at the critical section [IS:13920, 1993]. Based on constant overstrength moment capacity M_Ω over L_p [Paulay and Priestley, 1992] and identical parabolic distributions of total lateral force V and design base shear V_B along height of wall, V is estimated as,

$$V = M_\Omega V_B / M_D, \tag{1}$$

where M_D is the design bending moment [Dasgupta, 2008]. The components of V, i.e., $Q_{\Omega 1}$, $Q_{\Omega 2}$, $Q_{\Omega 3}$,

$Q_{\Omega 4}$, $Q_{\Omega 5}$, and $Q_{\Omega 6}$ are applied as uniformly distributed forces at floor levels (Figure 3c), along with unfactored vertical force $P_{ov,ext}$. Variation of $P_{ov,ext}$ during earthquake shaking is not considered.

Soil flexibilities along vertical, in-plane and out-of-plane directions are modeled by smeared springs at the bottom face of footing [CSI, 2006]. Along vertical direction, modulus of subgrade reaction below rectangular footing k_{sub} is obtained from ultimate bearing capacity of soil σ_{bc} and maximum vertical deflection Δ_{max} below toe of footing. Along other directions, k_{sub} is considered as 25% of the value in vertical direction [Das, 1999]. Soil anchors are required at suitable locations to reduce uplift and mobilise flexural strength under estimated $P_{ov,ext}$ and V (Figure 3c). At those locations, vertical translational nodal DOFs are restrained at bottom face. Absence of overhang in tapered geometry causes rigid block-type behavior of wall-footings and linear vertical displacement profiles in all types of soils (Figure 4a). Consequently, shear stresses are observed to be independent of soil flexibility (Figure 4b). Uniform variation of stress demand is obtained with increasing in-plane angle of taper α_{tX}. Subsequent analyses are carried out with properties of dry dense sand as strong soil [Dasgupta, 2008]. Passive pressure of backfill and soil compressibility are not considered in the analyses.

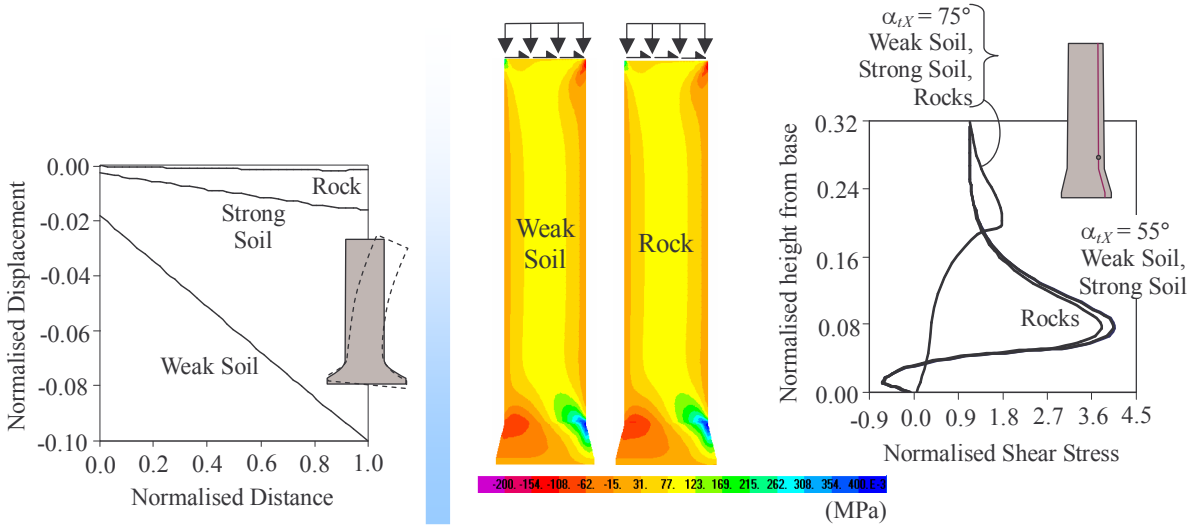

Figure 4 (a) Vertical displacement profile at the bottom; (b) averaged shear stress contours, and vertical shear stress distribution near the edges of wall-footings.

4.1. Configuration

In investigation of configuration, length of wall L_w, height of wall H_w, thickness of wall t_w, thickness of footing t_f and height of taper H_t are kept constant. The investigated wall-footings consist of (a) curvilinear tapers with degrees n_d of curve as 1.0, 1.25, 1.5, 1.75, 2.0 and 3.0, and (b) combined tapers with linear profile followed by curves of n_d = 1.5, 2.0 and 3.0 respectively. In walls with combined taper, α_{tX} becomes the starting angle of taper at the bottom (Figure 3b); thus, it depends on taper ratio r_t. Shear stress demand τ is monitored along a curve located at a distance of t_w inside the tapered edge and in central vertical plane of wall. In wall-footing with linear taper, τ increases steeply below the transition point due to stress concentration at re-entrant corner. With increasing n_d, profiles tend to take the shape of footings with sharp re-entrant corners, and intensity of τ increases towards the edges (Figure 5a). The beneficial characteristics of walls with linear taper (i.e., reduction of damage at bottom) and higher n_d (i.e., low τ in transition region) are combined in wall-footings with combined taper. Combined taper of n_d = 1.0 & 2.0 is selected for further investigations because this combination eliminates stress concentration in transition region and performs reasonably well at bottom region.

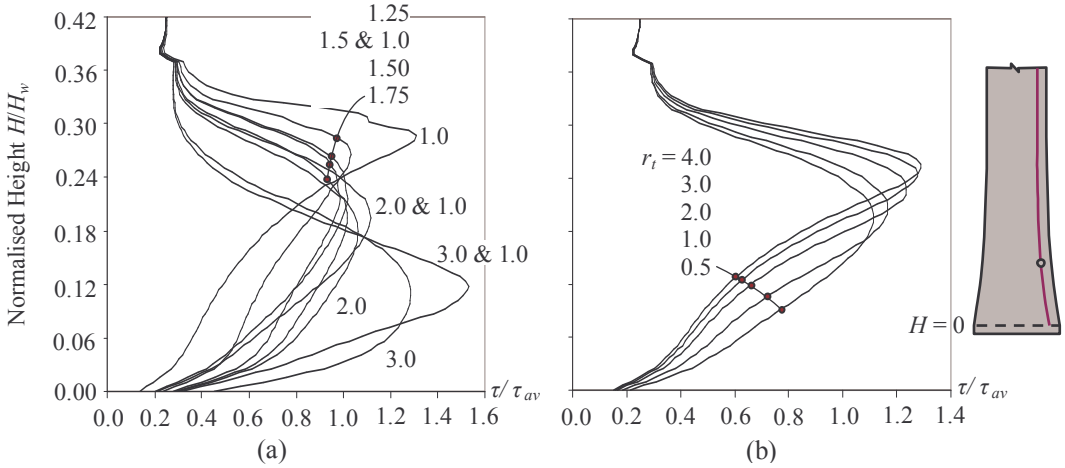

Figure 5 Variation of shear stress demand with (a) degree of taper and (b) taper ratio.

In investigation of influence of r_t on wall response, walls are analysed with r_t = 0.5, 1.0, 2.0, 3.0 and 4.0. In-plane and out-of-plane angles of taper are obtained from slope continuity [Dasgupta, 2008]. Lower r_t limits ease and economy of construction of bottom linear taper. With increasing r_t, location of peak τ near tapered edge shifts upwards (Figure 5b). Towards the bottom of footing, maximum difference of 49% is observed in τ between walls of low and high r_t because of stress concentration in walls with low r_t. Although τ in walls with high r_t increases by 37% to that in walls with low r_t towards the top of taper, location of peak demand near ground level makes it a favorable option. From functional point of view, high r_t increases obstruction of space on the sides of wall due to more flaring of linear taper. This drawback of high r_t is not significant because most of the tapered portion is proposed to be below ground level. Thus, r_t of 3.0 is chosen in the present study.

Two new parameters are introduced to characterise the geometry of combined taper, namely (a) length factor α_L (= L_w/L_f), and (b) width factor α_w (= t_w/B_f). For a particular α_L and other geometric parameters, limits on α_{tX} are derived for three different criteria, namely (a) slope continuity of curvilinear taper, (b) contact of wall-footing with underlying soil (full or partial contact), and (c) maximum bearing pressure of soil below wall-footing not exceeding σ_{bc} [Dasgupta, 2008]. Influence of these parameters is investigated here in the following study.

4.2. Length Factor

Higher α_L leads to lower L_f and overall economy of construction of tapered wall-footings; here, wall-footings are analysed with length factor α_L = 0.6, 0.7, 0.8 and 0.9 under combined $P_{ov,ext}$ and V. Tapered geometry of wall with lower α_L causes concentration of τ (Figure 6a), with almost 70% reduction in τ between walls with α_L as 0.6 and 0.9. In bottom central region of wall, negative shear stresses increase with α_L because of reduction in available wall area. Principal compressive stress $\sigma_{com,p}$ does not show significant variation in edge region (Figure 6b). Local strengthening of wall-footing is required to account for irregular variation of τ at anchor locations [Dasgupta, 2008]. Higher α_L leads to lower cost of construction and τ in transition region. Distribution of τ becomes more irregular towards the bottom with higher α_L, and this increases its vulnerability to seismic damage. Thus, selection of α_L is a trade-off between the two.

Stress demands τ and $\sigma_{com,p}$ are compared with design shear strength τ_c and design flexural compressive strengths $\sigma_{b,com}$ of concrete respectively [Dasgupta, 2008]. Shear failure of concrete is

expected in tapered region (Figure 6a) because of low τ_c arising from design longitudinal steel requirement of IS:13920. Compression failure of concrete at design level is expected in the upper portion of tapered region (Figure 6b). Considering the trade-off between demand and ease of construction and the extent of damage at the bottom, recommended length factor of slender wall-footing is 0.7.

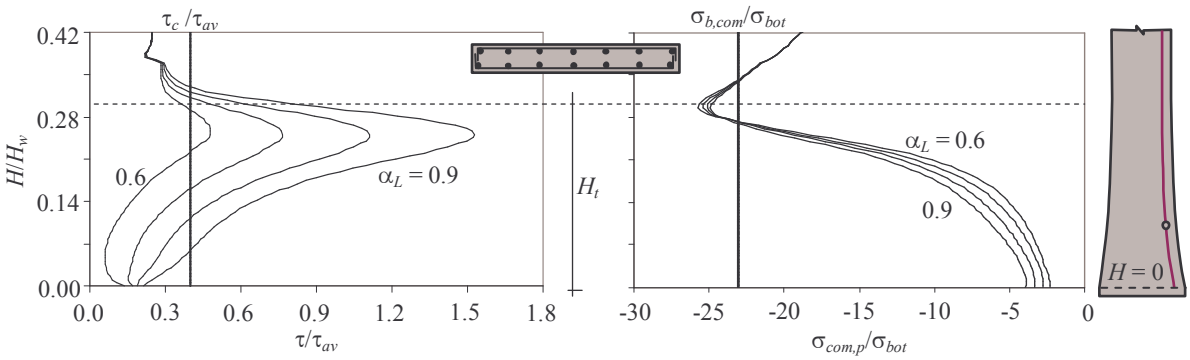

(a) (b)

Figure 6 Variation of stress demand and design strength with length factor for (a) shear and (b) principal stresses near tapered edge in central vertical plane.

4.3. Width Factor

Tapered wall-footings are analysed with width factor α_w (= t_w/B_f) as 0.11, 0.14, 0.2 and 0.33 respectively. With increasing width of wall-footing, shear forces are able to flow out into increased area resulting in more uniform distribution of τ near the edges (Figure 7a). In the central region, τ is not significantly affected by α_w [Dasgupta, 2008]. Except the upper portion of tapered region, $\sigma_{com,p}$ is observed to be less than the design strength (Figure 7b); with increase in α_w, intensity of $\sigma_{com,p}$ reduces towards the bottom as expected. Thus, higher α_w minimises possibility of seismic damage. Like in the study of α_L, comparison of τ and $\sigma_{com,p}$ with τ_c and $\sigma_{b,com}$ shows possibility of compression failure in upper portions of tapered region (Figure 7b). Possibilities of shear and compression failures may be minimised with suitable choice of α_w.

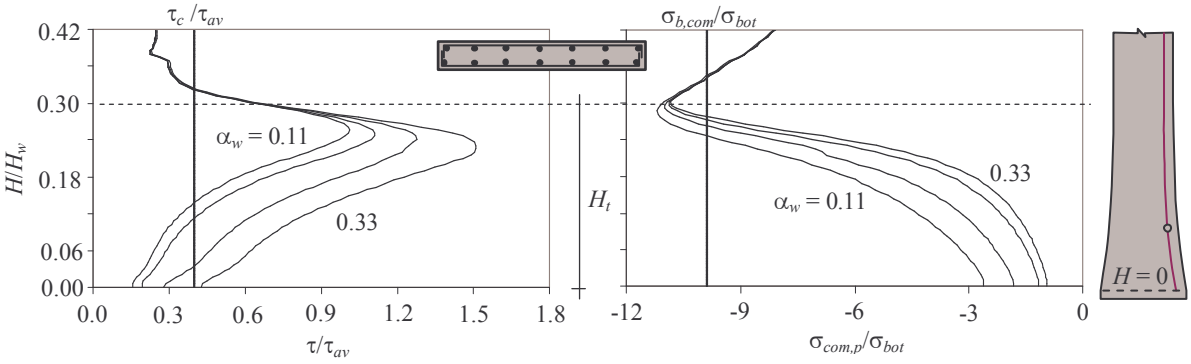

(a) (b)

Figure 7 Variation of stress demand and design strength with width factor for (a) shear and (b) principal stresses near tapered edge in central vertical plane.

Results of the above mentioned studies show that peak stress demand occurs at the upper portion of tapered region. Thus, seismic damage is likely to occur at that location with the rest of the tapered portion remaining linear elastic.

4.4. Angle of Taper

In RC wall-footing, direction of force flow at any point is given by angle of compression strut θ. At any point it is obtained as the inclination of principal compressive stress with the horizontal. Under concentrated vertical compression $P_{ov,ext}$ and lateral force V, the possible range of θ is 45°≤θ≤90°. Under combined action of distributed $P_{ov,ext}$ and V, proposed angle θ_p in bottom region is given as

$$\theta_p = \pi/4 + 0.5 tan^{-1}(P_{ov,ext}/V), \quad (2)$$

where $P_{ov,ext}$ is the unfactored vertical compression, and V overstrength shear demand at the critical section. With increase in α_L (i.e., decrease in L_f), force flow tends to get concentrated towards anchor locations. Also, in wall with low α_L more length of footing is available for forces to spread out. Thus, distribution of θ shifts on lower side with decreasing α_L near tapered edges (Figure 8). The proposed estimate θ_p is observed to be less than minimum strut angle θ_{min} (Figure 8); thus, θ_p may be considered as a measure of θ_{min}. Under different combinations of $P_{ov,ext}$ and V on slender walls, θ_{min}/θ_p is always observed to exceed α_{tX}/θ_p [Dasgupta, 2008]. Also, the range of variation of α_{tX}/θ_p is 0.9-1.2. Considering an average value of α_{tX}/θ_p as 1.0, α_{tX} may be estimated by Eqn. 2. Smooth flow of forces is ensured near tapered edges because α_{tX} is less than θ_{min}. Further investigations are required of possible modification of Eqn. 2 to account for inelastic wall response during earthquakes.

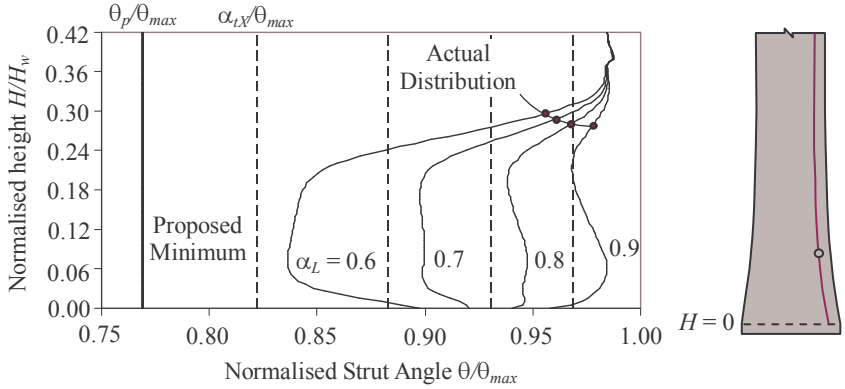

Figure 8 Comparison of proposed and actual strut angle distribution in tapered wall-footing.

5. CONSTRUCTION

Construction of tapered RC slender wall-footing involves construction of prefabricated tapered portion and straight vertical portion at site. To continue casting of straight portion, longitudinal reinforcement need to extend upto a distance of $1.5L_p$ above the top of precast portion; thus, splicing of reinforcement is eliminated in the inelastic region (Figure 9). Splicing of bars may be permitted beyond a height of $1.2L_p$ above the top of tapered portion. For any beam framing into tapered unit along in-plane or out-of-plane direction, bars need to be left in a similar way. Possible erection points, for lifting and placing the unit, may be located at the top surface, and lifting hooks attached at those locations. These are not shown in Figure 9.

6. CONCLUSIONS

The following salient conclusions can be drawn from the study:

(a) Combination of second order elliptic and linear tapers gives favourable stress response in the tapered region. Ratio of heights of linear to elliptic taper is recommended as 3.0.

(b) Tapered wall-footings are expected to be in partial contact with underlying soil during strong

earthquake shaking.

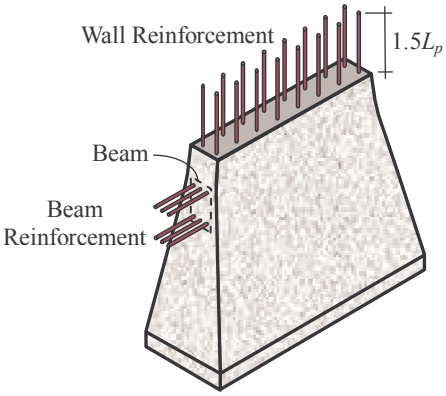

Figure 9 Precast tapered portion in RC wall-footing without enlarged boundary elements.

(c) Length factor of wall-footings is recommended as 0.7 for reasonable stress response.
(d) In wall-footings, starting angle of taper may be estimated as $\theta_p = \pi/4 + 0.5tan^{-1}(P_{ov,ext}/V)$ where, $P_{ov,ext}$ and V are unfactored vertical compression and overstrength shear demand on wall.
(e) Region of seismic damage in slender wall-footings is shifted above tapered region. Height of taper may be suitably chosen to determine the location of damage.
(f) Seismic damage in tapered region of slender RC wall can be achieved by making (i) maximum principal tensile stress to be significantly less than the cracking strength of concrete, and (ii) maximum principal compressive stress to be less than the design compressive strength.

7. ACKNOWLEDGEMENT

The authors gratefully acknowledge the financial support received from Ministry of Human Resource Development of the Government of India in carrying out the research work.

REFERENCE

CSI (2006). SAP2000: Integrated finite element analysis and design of structures. Computers and Structures Inc., California, USA.
EERI (1987). The San Salvador earthquake of October 10, 1986. *Earthquake Spectra* **3:3**, 543-562.
IS:1893 (Part 1)-2002 (2002). Indian standards criteria for earthquake resistant design of structures. BIS, New Delhi, India.
IS:13920-1993 (1993). Indian standard code of practice for ductile detailing of reinforced concrete structures subjected to seismic forces. BIS, New Delhi, India.
Kotronis, P., Ragueneau, F. and Mazars, J. (2005). A simplified modeling strategy for R/C walls satisfying PS92 and EC8 design. *Engineering Structures* **27**, 1197-1208.
Paulay, T., and Priestley, M. J. N. (1992). Seismic design of reinforced concrete and masonry buildings. John Wiley and Sons Inc., New York.
Dasgupta, K. (2008). Improvement in geometric design of reinforced concrete structural walls to resist earthquake effects. PhD Thesis, Indian Institute of Technology Kanpur, India.
Das, B. M. (1999). Principles of foundation engineering. Fourth Edition, Brooks/Cole Publishing Co., California, U.S.A.
Gajan, S., and Kutter, B. L. (2008). Capacity, settlement, and energy dissipation of shallow footings subjected to rocking. *ASCE Journal of Geotechnical and Geoenvironmental Engineering* **134:8**, 1129-1141.
Allotey, N., and El Naggar, M. H. (2008). An investigation into the Winkler modeling of the cyclic response of rigid footings. *Journal of Soil Dynamics and Earthquake Engineering* **28:1**, 44-57.